Journal of Current Science and Technology, May-August 2021 JCST Vol. 11 No.2, pp. 287-298
ISSN 2630-0656 (Online)

Cite this article: Benchaphong, A., Hongthong, R., Benchanukrom, S., & Konkong, N. (2021, May). Determination of the secondary bending stress in cold-formed steel connection. *Journal of Current Science and Technology*, *11*(2), 287-298. DOI: 10.14456/jcst.2021.29

Journal of Current Science and Technology

Journal homepage: https://jcst.rsu.ac.th

Determination of the secondary bending stress in cold-formed steel connection

Apai Benchaphong[1], Rattanasak Hongthong[1], Sutera Benchanukrom[2], and Nirut Konkong[3*]

[1]Department of Civil Engineering, Faculty of Engineering, Rajamangala University of Technology Krungthep, Bangkok 10120, Thailand
[2]Faculty of Agricultural Technology and Industrial Technology, Phetchabun Rajabhat University Petchabun, Petchabun 76000, Thailand
[3]Irrigation Office 3 - Royal Irrigation Department, Phitsanulok 65000, Thailand

*Corresponding author; nirut.k@ku.th

Received 1 January 2021; Revised 26 April 2021; Accepted 4 May 2021;
Published online 27 May 2021

Abstract

The purpose of this analysis was to study the effect of bolt load transfers and geometric variables which influence the secondary bending stress factor of cold-formed steel bolt connections using the analytical method. The Neutral Line Concept (NLC) was a method for determining the effect of secondary bending in bolt connection, but some important factors were ignored, such as load transmission occurring at the middle row bolts, overlap stiffening due to the action of manufactured and bolt stiffness. There was an effect on the level of the secondary bending stress in the bolt-row. To obtain accurately the secondary bending stress factor, the Modified Neutral Line Concept (MNLC) was proposed. MNLC was modified from NLC by added ignoring factors to the process of calculating. The accuracy of MNLC was validated by finite element analysis. The results showed that the analytical method had a good correlation with the finite element analysis. The most critical points for secondary bending stress in a lap shear connection were in the outer bolt rows of the connection.

Keywords: *analytical method; bolt connection; cold-formed steel; load transfers; secondary bending stress.*

1. Introduction

Bolt connections are essential components of most cold-formed steel structures. Failure mode prediction in cold-formed steel connections is crucial for structural damage analysis. The failure modes, such as the bearing failure mode, can be predicted by the bearing stress and bypass stress distribution along the bolt hole of the connection (Hart-Smith, 1982). In Konkong and Phuvoravan (2017b), both the bearing stress and bypass stress distribution were modified using the stress normalization concept for predicting the stress-strain relationship surrounding the bolt hole.

Secondary bending stresses are due to the loading configuration as the service load, and the eccentric load due to bolt-plate interaction, as well as the load transfer through bolts are established in the connection. This stress has the potential to change the failure mode and affected the ultimate failure load. When the contact area between the bolts and the hole edge was decreased by bolt rotation caused by secondary bending, this resulted in a decrease in the bearing resistance capacity of the lap shear connection (Ekh & Schön, 2005). As well, the combined secondary bending stress and tension stress cause a deterioration in fatigue performance and the net-tensile strength capacity (Ekh & Schön, 2005; Skorupa, Korbel, Skorupa, & Machniewicz, 2015). In other recent research, finite element analysis was used to investigate the secondary bending stress distribution throughout the thickness of plates in the surroundings of the

bolt-hole. The results showed that a non-uniform secondary bending stress distribution was found in the surroundings of the bolt-hole, in multi-bolt connections, and this reduced the bearing strength of the bolt-holes (Ireman, 1998; Egan, McCarthy, McCarthy, & Frizzell, 2012). One way to study secondary bending stress distribution is to measure the out-of-plane displacements along lines parallel to the loading direction, using a strain gauge. These measurements can be applied in the semi-empirical model for predictions of the fatigue life of the bolt connection. However, these measurements are complex and offer accuracy problems in regions of a higher stress gradient (Starikov, 2002; EKh, Schon, & Melin, 2005). The characteristics of secondary bending are dependent on the magnitude of the eccentricity and the flexural rigidity of the connection between the bolt rows. It was key to developing the Neutral Line Concept (NLC) for the secondary bending stress analysis (Schijve, 1972). NLC was a one-dimensional model in which the action of the relationship as a single structural entity was determined by the out-of-plane displacement of the neutral axis. Even though NLC was a useful method for determining the effect of secondary bending in eccentric bolt connection, but it ignores some important factors, such as stress concentration around bolt holes, load transmission occurring at the middle bolts row, overlap stiffening due to the action of manufactured and bolt stiffness. By ignoring factors, the NLC result in the multi-bolt-rows connection showed the maximum secondary bending stress in the outer bolt row and not presented the secondary bending stress in the middle row bolts (Machniewicz, Korbel, Skorupa, & Winter, 2018). It provides an inaccurate value and should be improved.

2. Objectives

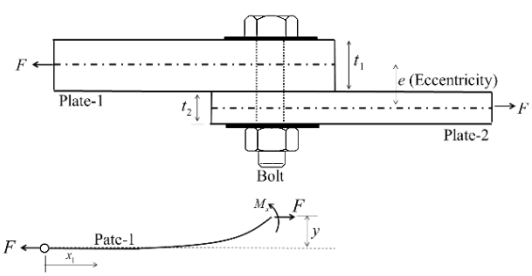

Figure 1 Eccentricity at bolt connection

In this research, NLC (Schijve, 1972) was modified by adding the bolt-plate interaction stiffness to the process of calculating. The modified method was called the Modified Neutral Line Concept (MNLC). The research was conducted by finite element analysis method and analytical method. The analytical method was used to consider the effects of the secondary bending stress as a function of the bolt load transfers which included bolt-plate interaction stiffness. The analytical result was compared by finite element analysis (FEA). In analytical and finite element analysis, the triple bolt single lap shear connection was used to illustrate the bolt load transfers and bolt stiffness influence the secondary bending stress.

3. Materials and methods

NLC was modified by including the bolt-plate interaction stiffness into the original analytical procedure which can be improved the load transmission occurring at the middle row bolts. The research procedure was focused on the multi-bolt-row connection which can be presented the bending stress behavior of the middle bolt row. The triple bolt lap shear connection with a 1 mm cold-formed steel plate and 5 mm steel bolt was a reasonable option for the multi-bolt-row connection. Because it was a simple model that achieves the research goal.

3.1 The secondary bending stress and the neutral line model

In Figure 1, the load path eccentric was presented in the geometry model. As a result of eccentric load, the bending moment of the plates was activated which is mentioned in the secondary bending stress. The severity of secondary bending stress was often calculated by the bending stress factor which can be defended by Eq. 1. The bending stress level at the critical location of the connection was not more than 3 times the tension stress ($S_b \leq 3$) (de Rijck, 2005).

$$S_b = \frac{\sigma_{bending}}{\sigma_{tensile}} \quad (1)$$

where S_b is the secondary bending stress factor, $\sigma_{bending}$ is the secondary bending stress and $\sigma_{tensile}$ is the tensile stress.

In 1972, Schijve proposed the analytical method of measure the secondary bending stress in the bolt connection which was calculated by considering the out-of-plane displacements of the

neutral line of the connection. In Figure 2, the structural components of the steel plate, and the steel bolt were determined on the assumption that the connection neutral line was a single beam. The overlap region of the top and bottom plates was considered as an integral beam in which the flexural rigidity corresponds to the combined thickness of the plates. However, some important factors were ignored such as stress concentration around bolt holes, load transmission occurring at the middle row bolts, overlap stiffening due to the action of manufactured and bolt stiffness. In this research, some components such as load transmission occurring at the middle row bolts and bolt-plate interaction stiffness were used to modify the NLC.

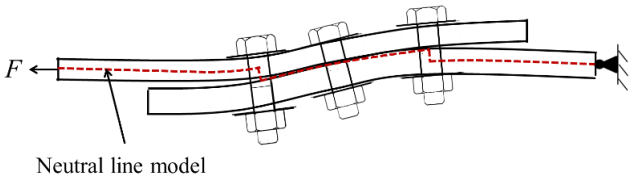

Figure 2 The original neutral line concept

3.2 An analytical method for the secondary bending stress analysis

In triple bolt connection (Figure 3(a), the bending moments at any point *x* along part-1 and part-2 were calculated by the differential of the deflection curve at the mid-plane surface (Figure 3(b)). The bending moment due to the deflection of the neutral line model was calculated as the moment-curvature relationship (Eq. (2)) (Timoshenko, 1922).

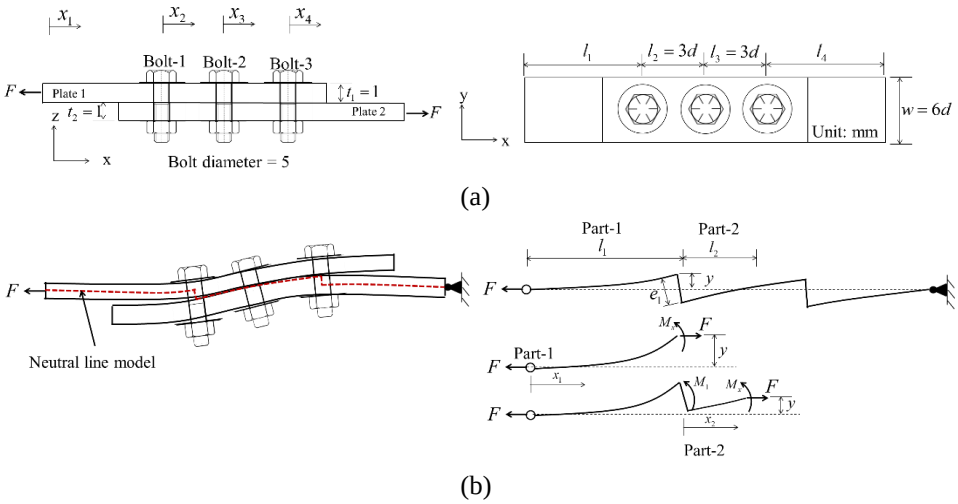

Figure 3 The multi-bolt-row connection analysis: (a) triple bolt connection; (b) neutral line model (Figure adapted from de Rijck, 2005)

$$M_i(x_i) = (EI)_i \left(\frac{d^2 y_i(x_i)}{dx_i^2} \right) \quad (2a)$$

with

$$M_i(x_i) = M_{i,A} + V x_i + \sum \Delta M_i + F\left(y_i(x_i) - y_i(0)\right) \quad (2b)$$

where F is the applied load, V is the shear force, $(EI)_i$ is the flexural stiffness of part-i, $M_{i,A}$ is the moment of point-A and i is the number of segments. The general solution of Eq. (2a) can be written as Eq. (3) (Timoshenko, 1922). The plate boundary conditions, $M_{i,A}$, $M_{i,B}$ and V are equal to zero.

$$y_i(x_i) = A_i \sinh(\alpha_i x_i) + B_i \cosh(\alpha_i x_i) + C_i x_i + D_i \quad (3)$$

where $\alpha_i^2 = F/(EI)_i$, $C_i = -V/F$ and $D_i = -M_{i,A}/F$.

In Figure 3(b), the equation for the deflection of the part-1 was similar to Eq. (3) which applied boundary conditions, as $y_1(x_1 = 0) = 0$, and it found that $B_1 = 0$. Thus, the equation $y_1(x_1)$ can be written as Eq. (4). The equation for the deflection the part-2, including load transfers and bolt stiffness can be written as Eq. (5).

$$y_1(x_1) = A_1 \sinh(\alpha_1 x_1) \quad (4)$$

$$y_2(x_2) = A_2 \sinh(\alpha_2 x_2) + B_2 \cosh(\alpha_2 x_2) - \frac{\Delta M_1}{F} \quad (5)$$

with

$$\Delta M_i = -M_i + M_{T,i},\ i = 1,2,3$$

$$M_{T,1} = \frac{(t_1 + t_2)}{2} T_1,\ M_{T,2} = \frac{(t_1 + t_2)}{2} T_2,$$

$$M_{T,3} = (F - T_1 - T_2)\frac{(t_1 + t_2)}{2} \text{ (when } T_3 = T_1)$$

where ΔM_i is an additional moment, M_i is the internal moments and $M_{T,i}$ is the moment from the transferred load (T_1, T_2 and T_3) (Figure 4).

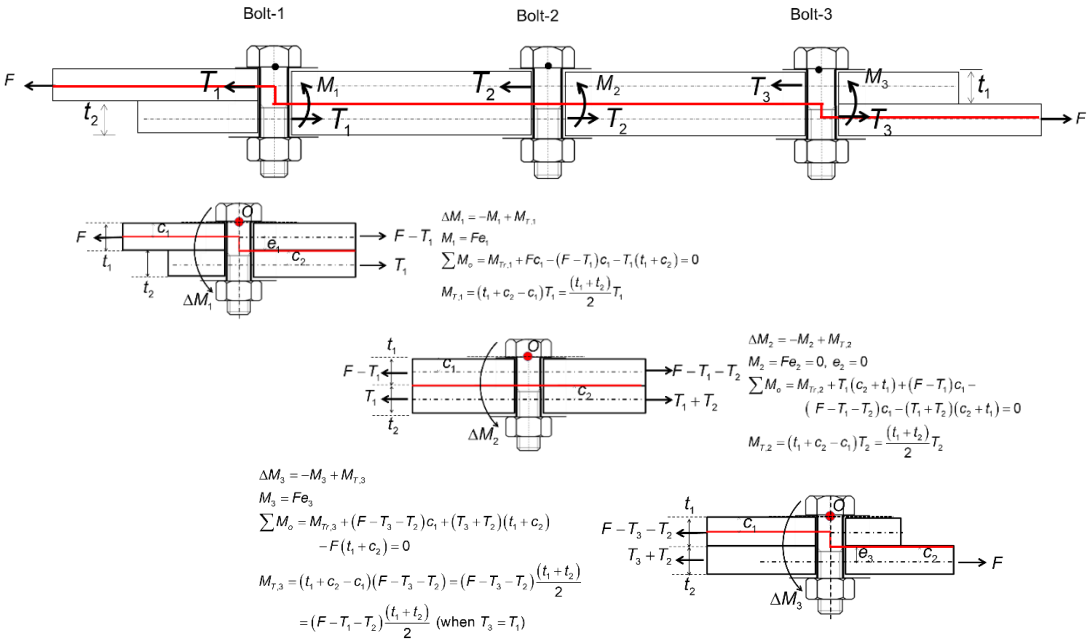

where t_1, t_2 = thickness of the plate, c_1, c_2 = distance to the neutral line, e_1, e_2 and e_3 = eccentricity and F = applied load.

Figure 4 Neutral line model and bending moments on the bolt rows for a three-row lap joint

The constant amplitude values of A_i and B_i of Eq. (3) were solved by the equilibrium equation with the boundary conditions (Timoshenko, 1922) at both the part 1- part 2 intersection and the connection hinged end. (Eq. (6)-(7)).

$$(y_{x,2})_{x_2 = L_2} = (y_{x,1})_{x_1 = L_1} + e_1 \quad (6a)$$

$$\left(\frac{dy}{dx}\right)_{x_1 = L_1} = \left(\frac{dy}{dx}\right)_{x_2 = 0} \quad (6b)$$

$$(y_{x,2})_{x_2 = L_2} = 0 \quad (7)$$

The constants A_1, A_2 and B_2, used in the above equations, are calculated in Eq. (8)

$$B_2 = A_1 \sinh(\alpha_1 L_1) + \frac{\Delta M_1}{F} + e_1 \quad (8a)$$

$$A_2 = \frac{\alpha_1}{\alpha_1} A_1 \cosh(\alpha_1 L_1) \quad (8b)$$

$$0 = A_2 \sinh(\alpha_2 L_2) + B_2 \cosh(\alpha_2 L_2) - \frac{\Delta M_1}{F} \quad (8c)$$

These constants were substituted in Eq. (2) and the bending moment along the length of the connection was calculated by Eq. (9).

$$M_x = EI_x \left(\frac{d^2 y_{\Delta m_i}(x)}{dx^2} \right) \quad (9)$$

Finally, the secondary bending stress factor in Eq. (1) was rewritten as Eq. (10).

$$S_b = \frac{\sigma_{bending}}{\sigma_{tensile}} = \frac{6M_x}{wt_1^2} \Big/ \frac{F}{wt_1} = \frac{6EI_x}{Ft_1} \left(\frac{d^2 y_{\Delta m_i}(x)}{dx^2} \right) \quad (10)$$

In Figure 5, the bolt load transfers were simplified by the multi-spring model. The k_2, k_5 and k_8 were the bolt-plate interaction stiffness which proposed by Konkong & Phuvoravan (2017a).

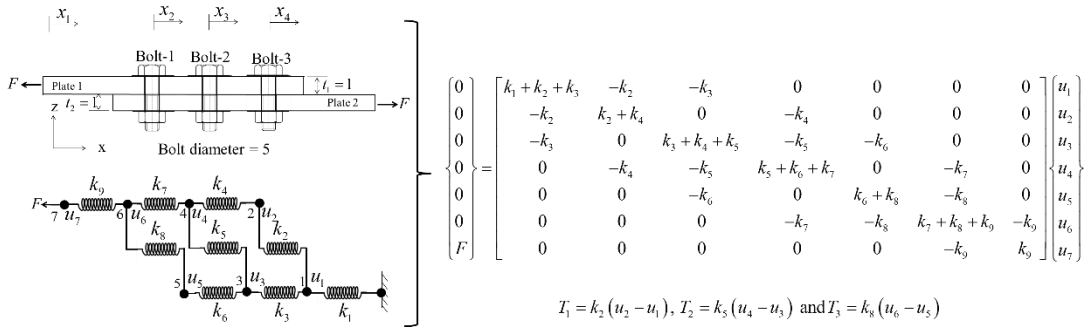

Remark: k_1 and k_9 are the stiffness of the plate from the bolt to the ends of plates, k_3, k_4, k_6 and k_7 are the stiffness of the plate between bolts.

Figure 5 The multi-bolt-row spring model (Figure adapted from Konkong & Phuvoravan, 2017a)

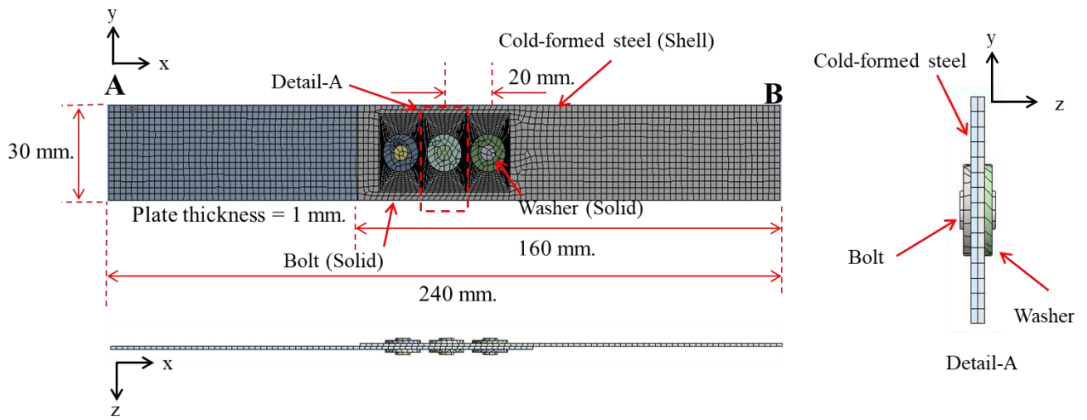

Figure 6 Geometry and element type of FEA

3.3 Finite element analysis

The ANSYS finite element program (ANSYS, 2014) was selected to analyze the cold-formed steel multi-bolt-row connection (Figure 6).

The material nonlinearity, nonlinear geometry and contact problem were adopted in the bolt connection geometry.

The material non-linearity, the true stress (σ_{true}) and true strain (ε_{true}) data were converted by the test stress-strain by Eq. (11) and were placed into the material model (Figure 7) The multilinear isotropic hardening material model and the linear elastic material model were used modeled the cold-form steel material and bolt-washer parts. The mechanical properties of the cold-formed steel and the steel bolts test procedures were followed ASTM (ASTM A370-07, 2007; A325M-94, 1994). The summary results of cold-formed steel and the steel bolts were presented in Table 1.

$$\sigma_{true} = \sigma_{test}(1 + \varepsilon_{test}) \text{ and } \varepsilon_{true} = \ln(1 + \varepsilon_{test}) \quad (11)$$

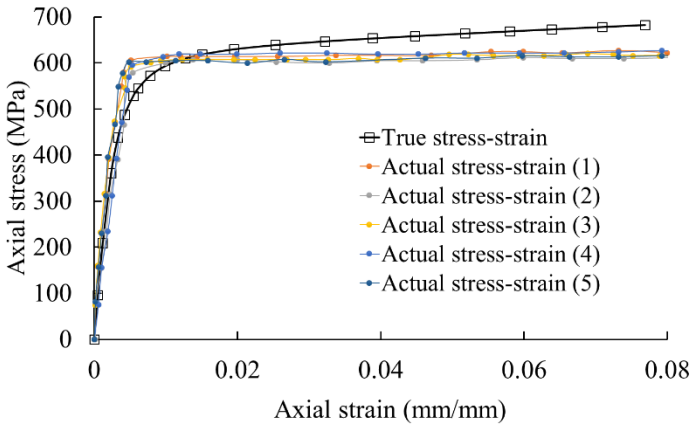

Figure 7 Stress-strain curve of cold-formed steel

Table 1 Material properties

Cold-formed steel				
***t* (mm)**	***w* (mm)**	F_y **(MPa**	F_u **(MPa)**	E **(GPa)**
1.05	12.60	608.79	624.99	213.52
Remark: ASTM A370-07b				
Steel bolt				
***d* (mm)**		F_y **(MPa**	F_u **(MPa)**	E **(GPa)**
4.94		930.79	952.38	204.10
Remark: ASTM A325M				

The SHELL 281 and SOLID186 were used to model the cold-formed steel and bolt-washer. The CONTA173 and TARGE170 were used to the contact elements that intended to model the contact between the steel plates, steel bolts, washers and wall of the holes (Figure 8). The penalty algorithm was considered to solve the constrained optimization of the contact element. The static friction in the contact element between the steel plates was set at 0.20 (Chung & Ip, 2000).

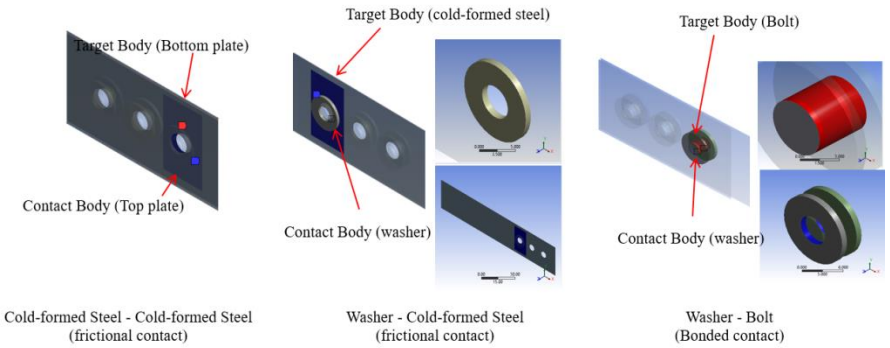

Figure 8 Contact body of finite element model

The aspect ratio of a geometric mesh shape (length-to-width ratio) was used to control the mesh size of the element which was assigned to be close to 1.0 for all components. The fine mesh was applied at the bolt holes which was predetermined to provide more accurate stress distribution (Chanamai & Rodkwan, 2019). The pins and the roller support were simulated to the boundary conditions on both sides of the connection (Figure 9).

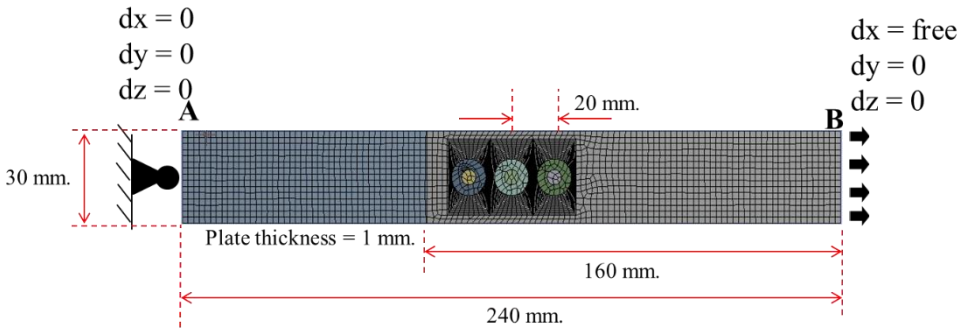

Figure 9 Mesh and boundary condition

The bending stress results of the cold-formed steel plates were considered by integrating the stress tensor. The shell bending stress tensors (σ_{xx}^{b}, σ_{yy}^{b} and σ_{xy}^{b}) are explained in the n-plane stress tensors ($\sigma_{xx}(z)$, $\sigma_{yy}(z)$ and $\sigma_{xy}(z)$) along the shell thickness direction. These can be written as Eq. (12).

$$\sigma_{xx}^{b} = \frac{6}{t^2}\int_0^t \sigma_{xx(z)}\left(\frac{t}{2}-z\right)dz,\ \sigma_{yy}^{b} = \frac{6}{t^2}\int_0^t \sigma_{yy(z)}\left(\frac{t}{2}-z\right)dz$$
$$\text{and } \sigma_{xy}^{b} = \frac{6}{t^2}\int_0^t \sigma_{xy(z)}\left(\frac{t}{2}-z\right)dz \quad (12)$$

where σ_{xx}^{b}, σ_{yy}^{b} and σ_{xy}^{b} are shell bending stress, t is the total shell thickness and z is the thickness location where the in-plane stress is evaluated (ANSYS, 2014).

4. Results

The analysis results of the analytical method were verified by the finite element model as shown in Figure 10(a-c). The results provide a continuous curve of the variation of the bending stress level and bending stress factor along the length of the connection.

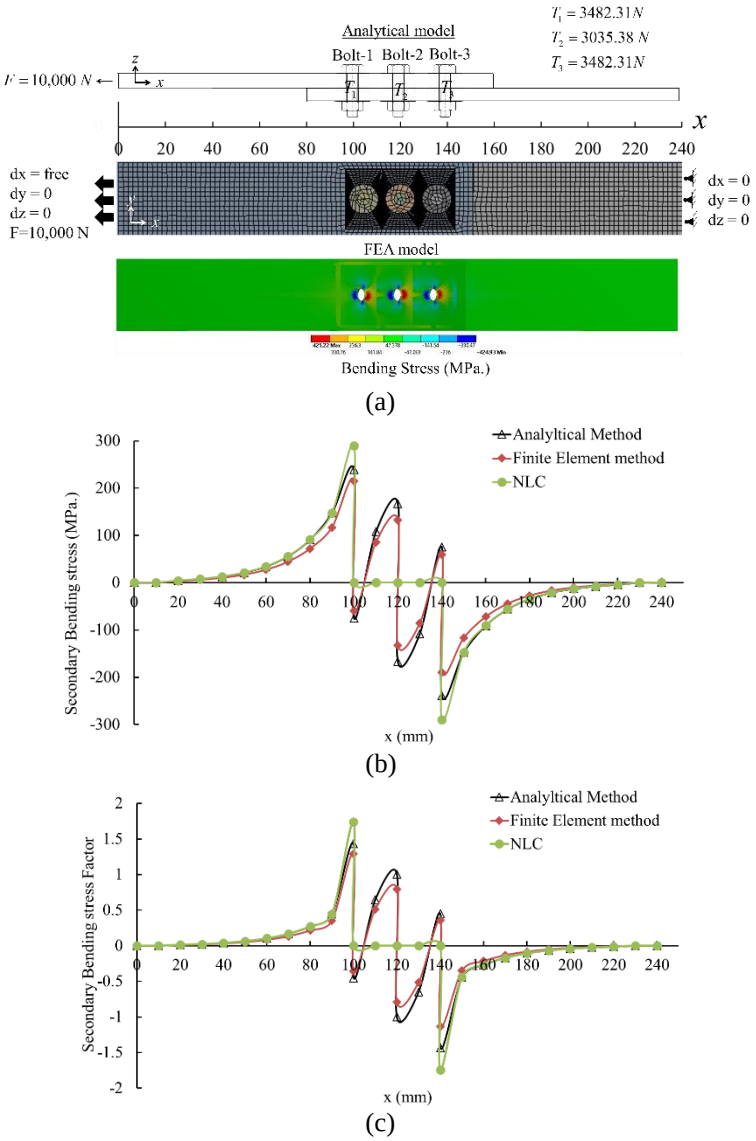

Figure 10 Variations of the bending stresses and bending stress factor along the lap shear connection: (a) FEA model; (b) secondary bending stresses; (c) secondary bending stress factor

The results show that the analytical method was in good correlation with the FEA although it a few differences with NLC due to various assumptions. In NLC, the load transmission occurs at the outer bolts only and does not transfer to the bolts in the middle row because bolt-plate interaction stiffness was ignored. In MNLC, bolt-plate interaction stiffness was added to the NLC that affected the load transmission from one plate to the other plate and occurred by all three rows, also the middle row. The most critical points for bending stress in a lap shear connection were bolt-row-1 and bolt-row-3 of the connection as shown in Figure 10(a). The region along the bolt-row-1 and bolt-row-3 were the high secondary bending stress. These were a

primary concern for bending failure analysis. At the bolt-row-2 location, the secondary bending stress along the connection width was minor which little interest for bending failure behavior.

5. Analytical parametric study of the bolt connection

Some parameters have been influenced by the secondary bending stress of the connection. The parametric study considered the secondary bending stress with variations in the bolt diameter, plate thickness ($t = t_1 = t_2$) and plate thickness ratio (t-ratio, t_2/t_1). The geometric model, discussed above, was modified for the various parameters being analyzed.

Changing the bolt diameter had a significant effect on the secondary bending stress factor in a multi-bolt-row connection that increased the peak secondary bending stress of the region along the outer bolt rows. Increasing the bolt diameter examined the influence of the bolt-plate interaction stiffness which induced higher values of the transfer load level (T_1 and T_3) and the additional moment (ΔM_1 and ΔM_3), which resulted in a high secondary bending stress factor (Figure 11).

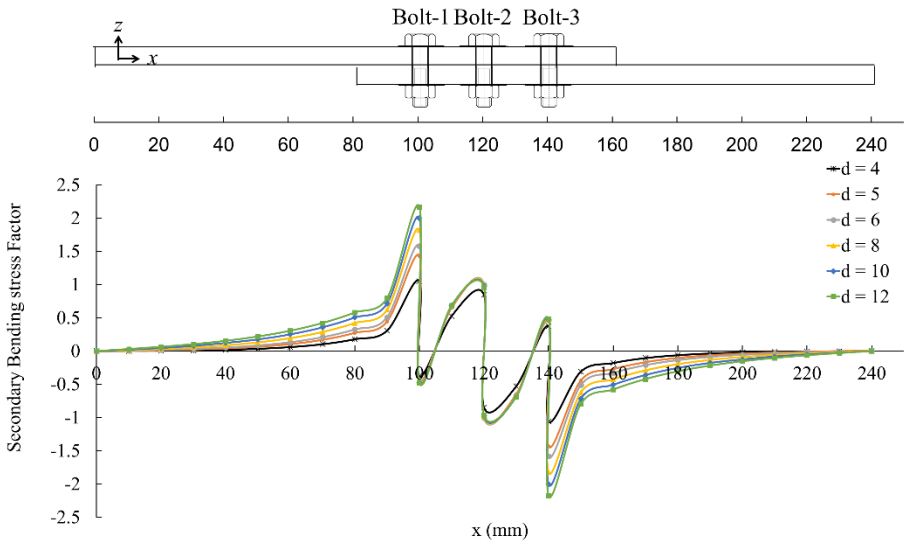

Figure 11 Secondary bending stress factor results of varying bolt diameters

When the cold-formed steel plate thickness changed to be very thin plates, the bending stiffness and axial stiffness of the plate were reduced to being very small. This resulted in the plates at the outer bolt rows being unable to resist the secondary bending moment, and a larger axial deformation occurred, and high rotations occurred at the middle bolt row. When the plate thickness was decreased, the position of the high peak secondary bending stress factor changed to the region along the middle bolt row (Figure 12).

The secondary bending stress factor of the region along the bolt-1 was transcended when the t_2/t_1 ratio was greater than 1. While the t_2/t_1 ratio was greater than 1 ($t_2/t_1 \gg 1$), the steel bolt was constrained by the axial stiffness of the plate-2 which was semi-fixed support, and the secondary bending stress was carried by the region along the bolt-1 (Figure 13). The parametric results show that the increasing of bolt diameters plate thickness and plate thickness ratio has an impact on the secondary bending stress factor due to the bolt-plate interaction stiffness and the load distribution changed.

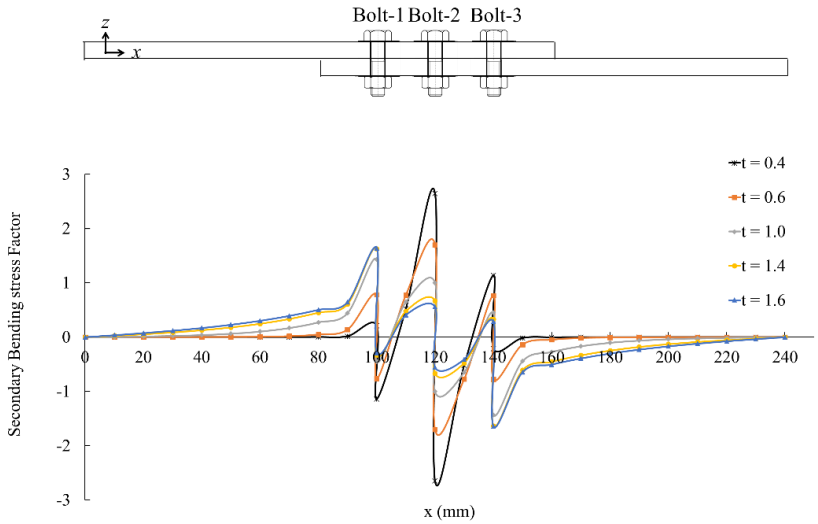

Figure 12 Secondary bending stress factor results in varying plate thickness

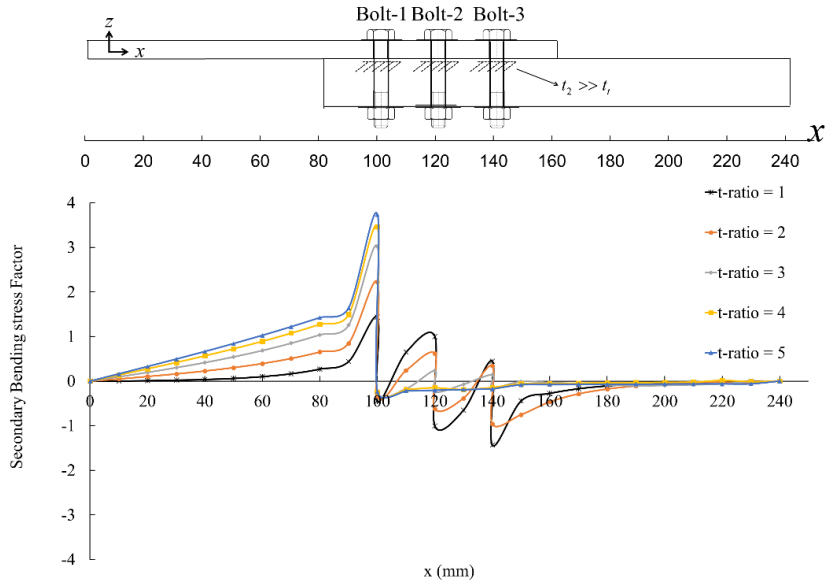

Figure 13 Secondary bending stress factor results in varying plate thickness ratio ($t_2/t_1 >> 1$)

6. Conclusion

The phenomenon of the secondary bending effect in triple-row bolt cold-formed steel lap shear connections was the focus of our study. The analytical method and the FEA were separately applied to study the secondary bending stress effects on the mechanical behavior of a lap shear bolt connection. The analytical method was a modified form of NLC which included the concept of load transfer. The results from the analytical method were verified by FEA. The analytical method was employed to calculate the secondary bending in the critical location of the connection. The accuracy of the results from the analytical method was verified by the FEA, with a high correlation between the two. The effect on the secondary bending stress of the region along with the bolt, of varying the parameters, was analyzed with the analytical approach. Varying the bolt diameters and the plate thickness ratio (t_2/t_1) showed that the high secondary bending stress is in the region along the outer bolt rows. When the plate thickness was decreased, a high level of secondary bending stress factor occurred in the region along the middle bolt row. The analytical method can be used to investigate the

secondary bending stress factor, which depends on the dimensions of the connection. Predicting the magnitude and location of peak secondary bending stresses were guided to fatigue analysis that occurred in regions of high secondary bending. Moreover, the modified neutral line model is a highly efficient tool to use in the early stages of connection analysis and design.

7. Acknowledgements

The authors wish to acknowledge the National Research Council of Thailand (NRCT) for providing funding support and Mr. Roy I. Morien, of the Naresuan University Graduate School, for his assistance in editing the English expression and grammar in this paper.

8. References

A325M-94. (1994). High strength bolts for structural steel joints [Metric], *ASTM International*, West Conshohocken, PA, 19428-2959 USA. www.astm.org

ANSYS. (2014). ANSYS user's manual Revision 15, *ANSYS, Inc*.

ASTM A370-07. (2007). Standard Test Methods and Definitions for Mechanical Testing of Steel Products, *ASTM International*, West Conshohocken, PA, 19428-2959 USA. www.astm.org

Chanamai, P., & Rodkwan, S. (2019). Numerical simulation of gas-solid flow in a cement precalciner using adaptive mesh refinement. *Journal of Current Science and Technology, 9*(2), 107-122. DOI: 10.14456/jcst.2019.11

Chung, K. F., & Ip, K. H. (2000). A general design rule for bearing failure of bolted connections between cold-formed Steel Strips. *International Specialty Conference on Cold-Formed Steel Structures*, 593-605.

De Rijck, J. J. M. (2005). *Stress analysis of fatigue cracks in mechanically fastened joints: An analytical and experimental investigation* (Doctoral thesis, Delft University of Technology, The Netherlands). Publisher Delft University Press 316 pp. Retrieved from https://www.narcis.nl/publication/RecordID/oai:tudelft.nl:uuid:c6253348-532d-4159-bb4c-00cb8a1f5c2b

Egan, B. T., McCarthy, C., McCarthy, M. A., & Frizzell, R. F. (2012). Stress analysis of single-bolt, single-lap, countersunk composite joints with variable bolt-hole clearance. *Composite Structures, 94*(3), 1038-1051. DOI: 10.1016/j.compstruct.2011.10.004

Ekh, J., & Schön, J. (2005). Effect of secondary bending on strength prediction of composite, single shear lap joints. *Composites Science and Technology, 65*(6), 953-965. DOI: https://doi.org/10.1016/j.compscitech.2004.10.020

Ekh, J., Schon, J., & Melin, L. G. (2005). Secondary bending in multi-fastener composite-to aluminum single shear lap joints. *Composites Part B: Engineering, 36*(3), 195-208. DOI: https://doi.org/10.1016/j.compositesb.2004.09.001

Hart-Smith, L. J. (1985). Bonded-bolted composite joints. *Journal of Aircraft, 22*(11), 993-1000. DOI: https://doi.org/10.2514/3.45237

Ireman, T. (1998). Three-dimensional stress analysis of bolted single-lap composite joints. *Composite Structures, 43*(3), 195-216. DOI: https://doi.org/10.1016/S0263-8223(98)00103-2

Konkong, N., & Phuvoravan, K. (2017a). An analytical method for determining the load distribution of single-column multi bolt connection. Advances in Civil Engineering. DOI: 10.1155/2017/1912724.

Konkong, N., & Phuvoravan, K. (2017b). Parametric study for bearing strength in cold-formed steel bolt connections. *International Review of Civil Engineering (I.RE.C.E.), 8*(3), 87-96. DOI: 10.15866/irece.v8i3.11850.

Machniewicz, T., Korbel, A., Skorupa, M., & Winter, J. (2018). Analytical, numerical and experimental investigation of the secondary bending of riveted lap joints. *AIP Conference Proceedings.* Volume 2028, Issue 1. DOI: https://doi.org/10.1063/1.5066400

Schijve, J. (1972). Some elementary calculations on secondary bending in simple lap joints, Report NLR TR 72036, Amsterdam

(Netherlands): NLR. National Technical Reports Library, https://ntrl.ntis.gov/NTRL/dashboard/searchResults/titleDetail/N7231911.xhtml

Skorupa, M., Korbel, A., Skorupa, A., & Machniewicz, T. (2015). Observations and analyses of secondary bending for riveted lap joints. *International Journal of Fatigue*, *72*, 1-10. DOI:

Starikov, R. (2002). Mechanically fastened joints - Critical testing of single overlap joints Scientific Report FOI-R-0441-SE. Stockholm, Swedish Defense Research Agency, Aeronautics Division, FAA

Timoshenko, S. P (1922). LXVI. On the correction for shear of the differential equation for transverse vibrations of prismatic bars," Philosophical Magazine, 41, 744-746. DOI: https://doi.org/10.1080/14786442108636264